General Disclaimer

One or more of the Following Statements may affect this Document

- This document has been reproduced from the best copy furnished by the organizational source. It is being released in the interest of making available as much information as possible.

- This document may contain data, which exceeds the sheet parameters. It was furnished in this condition by the organizational source and is the best copy available.

- This document may contain tone-on-tone or color graphs, charts and/or pictures, which have been reproduced in black and white.

- This document is paginated as submitted by the original source.

- Portions of this document are not fully legible due to the historical nature of some of the material. However, it is the best reproduction available from the original submission.

Produced by the NASA Center for Aerospace Information (CASI)

(NASA-CR-176015) MMIC DEVICES FOR ACTIVE PHASED ARRAY ANTENNAS Semiannual Report, 21 Dec. 1984 - 20 Jun. 1985 (Illinois Univ.) 18 p HC A02/MF A01 CSCL 17I
N85-30177
Unclas
G3/32 21741

MMIC DEVICES FOR ACTIVE PHASED ARRAY ANTENNAS

SEMIANNUAL REPORT

21 December 1984 to 20 June 1985

Supported by

Contract No. NASA NCC3-38
National Aeronautics and Space Administration
Lewis Research Center
Cleveland, Ohio 44135

June 1985

by
R. Mittra
Electromagnetic Communication Laboratory
Department of Electrical and Computer Engineering
University of Illinois
Urbana, Illinois 61801

JUL 1985
RECEIVED
NASA STI FACILITY
ACCESS DEPT.

MMIC DEVICES FOR ACTIVE PHASED ARRAYS

1. INTRODUCTION

During the past six months, considerable progress has been made in the calculation and measurement of the scattering parameters of printed circuit discontinuities.

These discontinuities occur in a variety of structures, such as transitions between rectangular waveguide and printed circuits, junctions between circuits of different dielectric constants, and filters and impedance matching circuits. Because of the variety of devices in which these discontinuities occur, it is very useful to understand them in as great a detail as possible.

As stated above, in this investigation we are considering both theoretical and experimental studies of discontinuities. The theoretical studies have focused on finding ways to predict the scattering from discontinuities. The experimental studies have concentrated on developing measurement techniques for determining the scattering parameters of these discontinuities. It is necessary to attack this problem from both points of view, since experimental verification will be needed for the theoretical results.

In this report we will present both experimental and theoretical results for a symmetrical double discontinuity in strip width. It will be seen that there is good agreement between the theory and experiment.

Since the theory has been described in a previous NASA report [1], we concentrate here on presenting the details of the experimental design, and demonstrating the agreement between the numerical and experimental results.

Let us proceed now to the experimental design.

2. DESIGN CONSIDERATIONS

In this section, a description of the design procedure for microstrip lines is given. A diagram of uniform microstrip is shown in Figure 1. The microstrip-line dimensions were determined using closed-form expressions derived by Hammerstad [2]:

For $W/h \leq 2$,

$$W/h = \frac{8 \cdot \exp(A)}{\exp(2A) - 2} \tag{1}$$

For $W/h \geq 2$,

$$W/h = \frac{2}{\pi} \cdot \left[B - 1 - \ln(2B-1) + \frac{\epsilon_r - 1}{2\epsilon_r} \cdot \left\{ \ln(B-1) + 0.39 - \frac{0.61}{\epsilon_r} \right\} \right] \tag{2}$$

where

$$A = \frac{Z_o}{60}\sqrt{\frac{\epsilon_r+1}{2}} + \frac{\epsilon_r - 1}{\epsilon_r + 1} \cdot (0.23 + \frac{0.11}{\epsilon_r})$$

$$B = \frac{377\pi}{2Z_o\sqrt{\epsilon_r}}$$

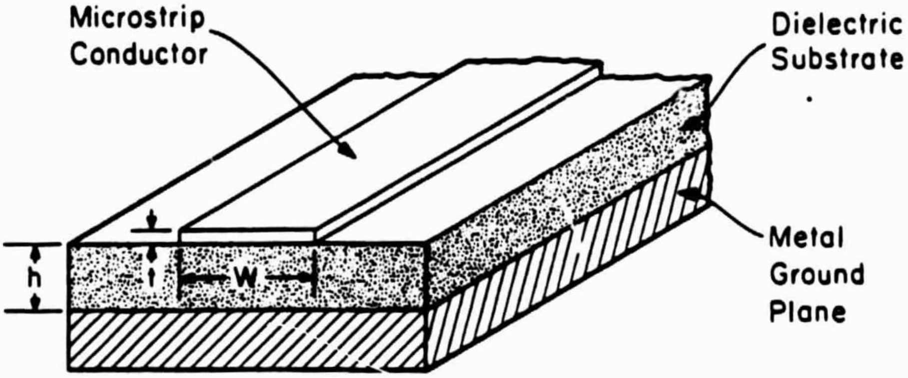

Figure 1. Microstrip cross-section.

A 50 Ω line on 0.031" thick Duroid and with a relative dielectric constant of 2.2 resulted in a strip width of 0.093". Table 1 shows the dimensions of microstrip lines with characteristic impedances of 100, 75, 50, 40 and 30 Ω based upon equations (1) and (2).

To complete the design, the length of the microstrips had to be determined. The dimensions of the circuit boards had to be small to minimize loss through the guide, while, at the same time, it had to be long enough to ensure that any perturbations in the guide fields were confined to the vicinity of the discontinuity under study. In addition, field perturbations, caused by the connectors and coaxial to microstrip transitions, had to be minimized. The attenuation constant for the lowest non-TEM mode was computed by Farr using a spectral Galerkin technique, and it proved to be greater than 50 dB/cm at 10 GHz [3]. For a 2 cm long section, this attenuation constant provided sufficient resolution between the individual step discontinuities. Figure 2 shows the microstrip lines used in the experiment. Sections with characteristic impedances of 100, 75, 40 and 30 Ω were inserted in series with the 50 Ω line; referring to Figure 2, note that lines C through F have 2 cm long center sections, whereas line B has a 1.25 cm center section. This line was used to show how isolation between discontinuities depended on their separation. The measuring system was based on a 50 Ω reference. Similarly, to isolate the discontinuity effects created by the connectors, line segments leading to the

Table 1

Microstrip design parameters with h = 0.031"

Z_o	W/h	W (inches)	ϵ_{eff}
30	6.23	.193	1.951
40	4.25	.132	1.907
50	3.08	.093	1.870
75	1.59	.049	1.805
100	0.89	.028	1.758

ORIGINAL PAGE IS
OF POOR QUALITY

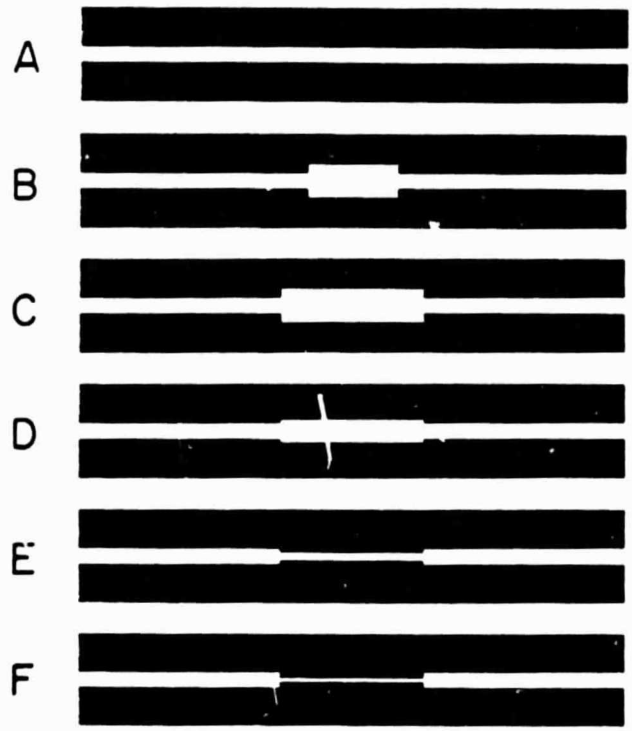

Figure 2. Microstrip patterns printed on Duroid: A) 50 Ω line, B) 30 Ω short section, C) 30 Ω section, D) 40 Ω section, E) 75 Ω section, F) 100 Ω section.

discontinuity were made 2.81 cm long. Thus, the overall length of the microstrips was 7.60 cm. For improved accuracy, the microstrips were etched using photolithography and were gold plated.

The test fixture, shown in Figures 3 and 4, was designed to within the specified tolerance of 0.002". A flanged seal was included for shielding and for simplicity in aligning the boards during assembly. The microstrip boards were firmly pressed against the ground plane to insure good electrical connection and uniform thickness. The connectors utilized belong to the Wiltron K-Connector series. The sparkplug female K102-F:SP42 connector proved to be ideal for this application due to its outstanding electrical and mechanical performances [4], [5]. As suggested by Oldfield [6], the center pins were custom made to provide for an optimum transition from the coaxial line to the microstrip. The custom-made center pins, supplied by Wiltron, had a diameter of 0.040" and were gold plated. It has been found that the diameter of the pin had to be equal, or no less than one-third the microstrip line width [7]. A good transition was obtained by soldering the 0.040" diameter pin onto the 0.093" wide microstrip line. In addition, a short section of the air line and a gap between the microstrip board and the wall of the fixture provided the required matching for the transition from coaxial cable to the microstrip. The air line was designed using the known result for coaxial cables [8]; the outer diameter of the 50 Ω line is 2.3 times the inner one. For a 0.040" pin, the outer diameter is 0.092". These simple modifications were recommended by Wiltron

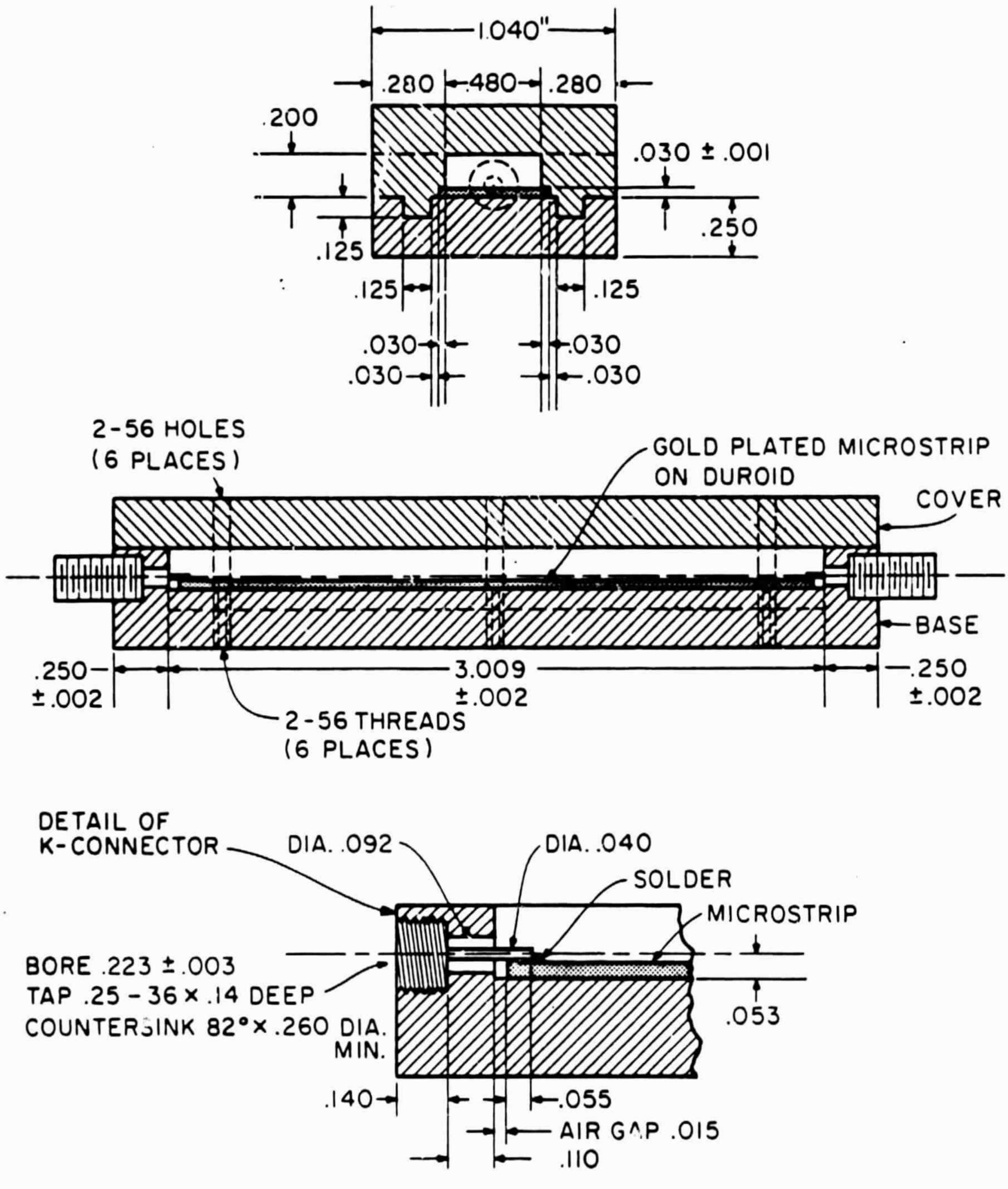

Figure 3. Machine drawing of test fixture. Note 0.015" compensation gap; this provides matching between connector and microstrip. All dimensions are in inches.

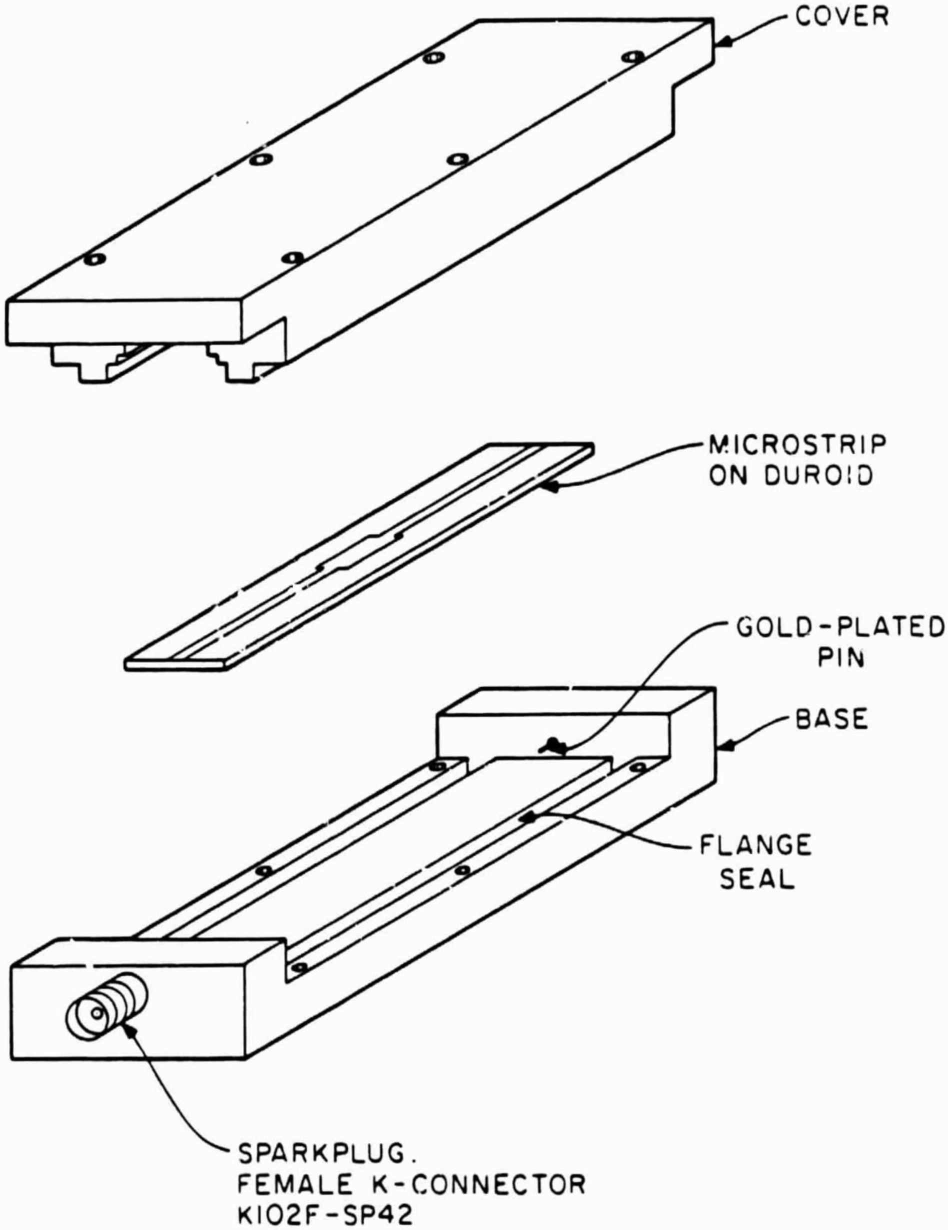

Figure 4. Assembly drawing of test fixture. Note flanged seal to avoid radiation to the outside. Also note that cover presses board tightly onto base.

in their assembly instructions [9]. To insure repeatability, the connectors were adjusted using a torque wrench.

3. MEASUREMENT PROCEDURE, RESULTS, AND COMPARISON WITH THEORY

A series of full band measurements for the various microstrip lines was carried out using an HP8510 network analyzer. The system was calibrated at 401 data points ranging from 45 MHz up to 18.045 GHz. The 18 GHz range contains all integer multiples of the 45 MHz fundamental frequency as required for computing the inverse Fast Fourier Transforms in the time-domain analysis.

A diagram of the experimental setup used to measure return loss is shown in Figure 5. This setup includes the HP8510 Automatic Network Analyzer, test jig, microstrip board, and 50 Ω load. This setup was used in a number of experiments with different boards, shown previously in Figure 2.

We now present selected results from these experiments. In Figure 6, the return loss is plotted as a function of frequency for a uniform 50 Ω line. Note that for most of the frequency range, the insertion loss is greater than 35 dB. This figure is indicative of the quality of the transition between the coax and microstrip lines. Also shown in Figure 6 is the reflection coefficient in the time domain. From this we again verify the quality of the transition, by noting that the reflection coefficient is less than .025 over most of the bandwidth.

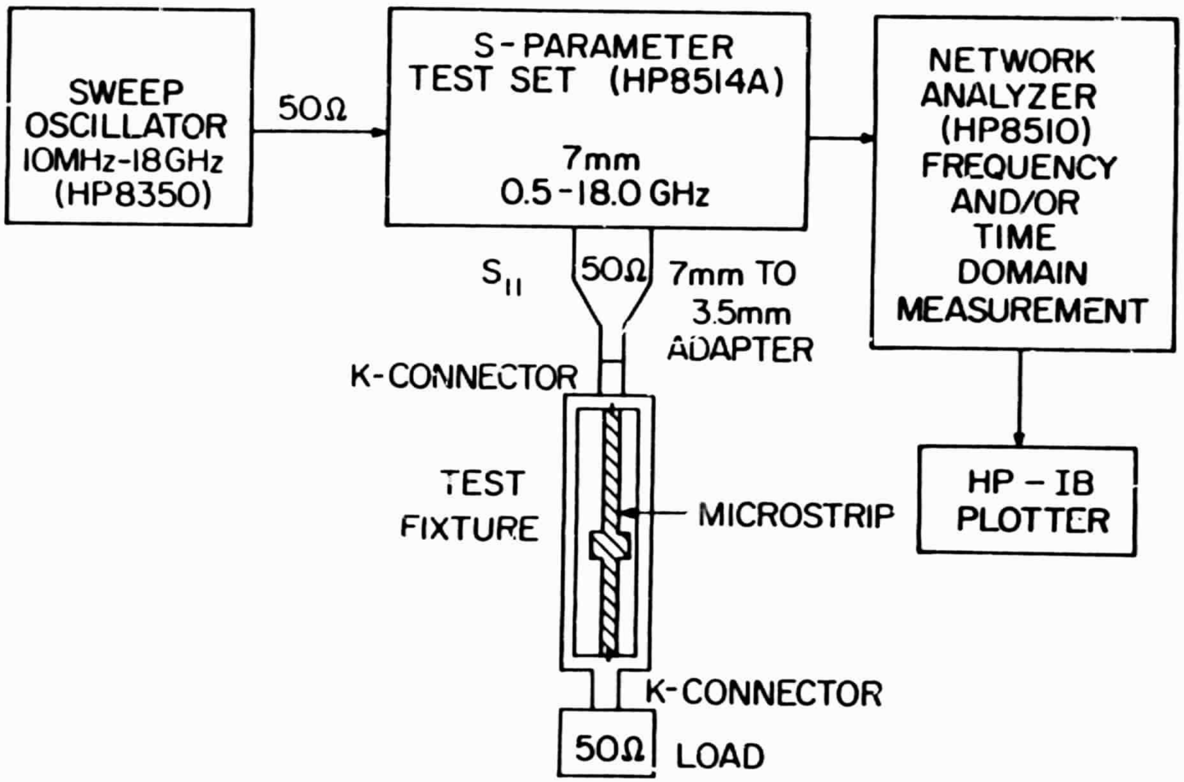

Figure 5. Block diagram of the test equipment used to measure the reflection coefficient and return loss of the microstrip lines.

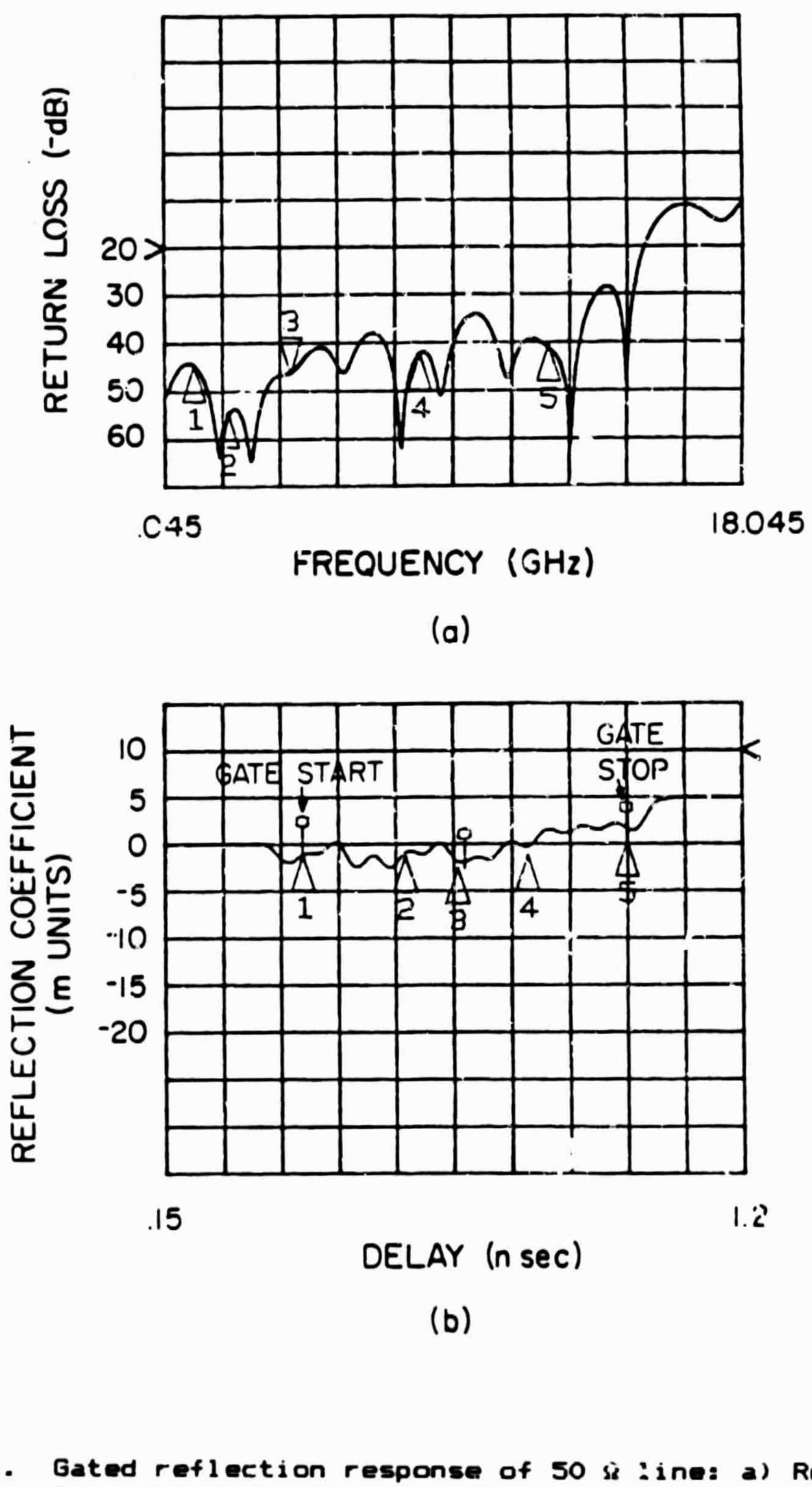

Figure 6. Gated reflection response of 50 Ω line: a) Return loss, b) Reflection coefficient.

Next, we present results for a microstrip line with a 30 Ω step in the middle, whose mask was shown previously in Figure 2c. The results, shown in Figure 7, again show the reflection coefficient in the frequency and time domains.

From plots such as these, we may compare the measured insertion loss at specific frequencies to those obtained with theory. These comparisons are shown in Table 2. The theories used for comparison are the mode matching procedure that is being worked on by Farr [3], and a simplified transmission line approach. The results from the two theories are in good agreement with each other, and with the measured values. We may therefore conclude that the results obtained by experiments are accurate to within a few percent of the predicted values.

4. CONCLUSIONS AND FUTURE WORK

With the results demonstrated in this report, we have demonstrated a method of measuring microstrip discontinuities to a high degree of accuracy. Furthermore, we have shown that these experimental results agree well with results generated from the theoretical methods that have been presented previously. With this correlation established, we may now study a variety of structures from both an analytical and theoretical point of view. These structures will include multiple cascaded sections, taper, and structures which include stepwise changes of the dielectric substrate as are encountered when interfacing with MMIC chips. In addition, work is being planned to study and characterize many

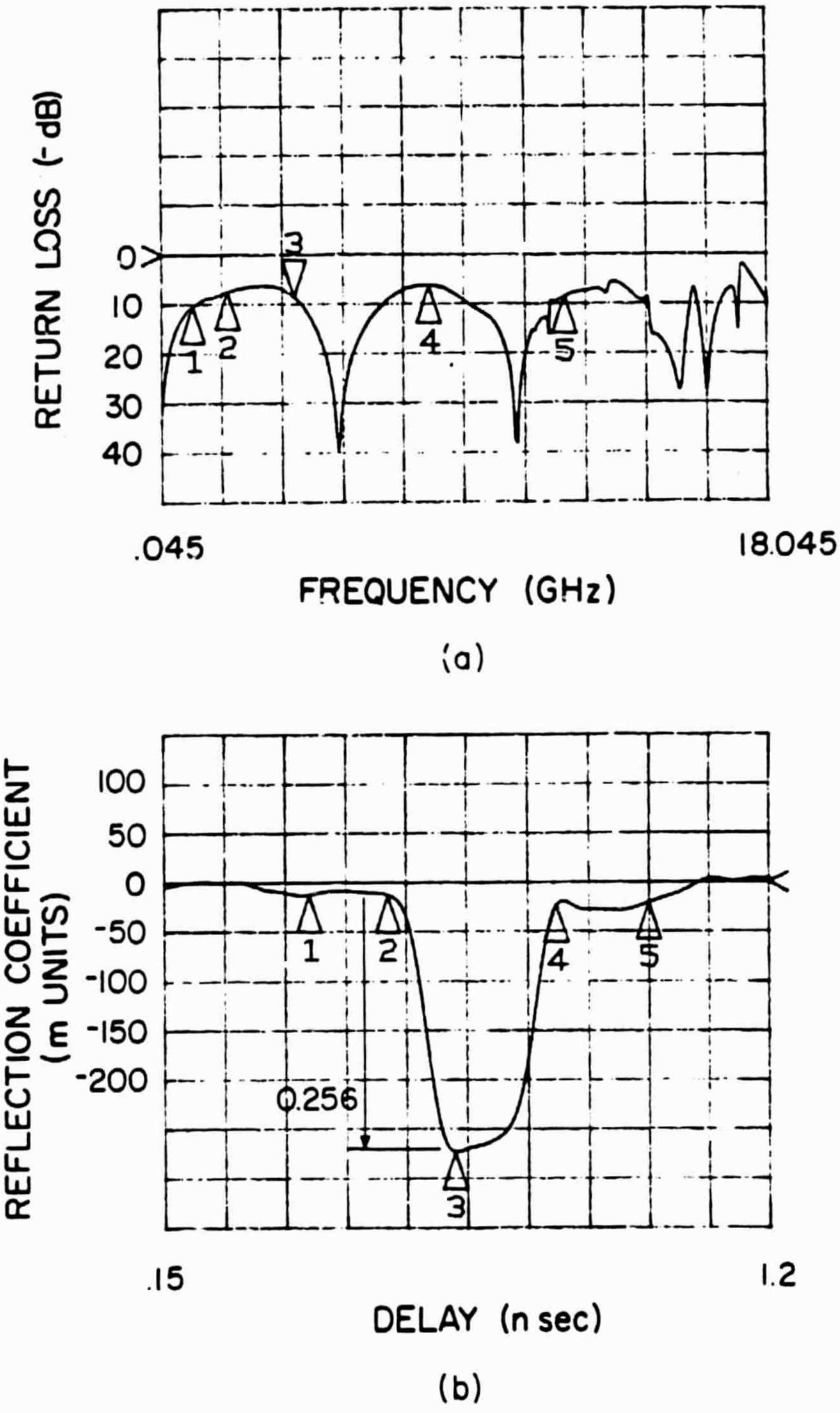

Figure 7. Reflection response of 30 Ω line: a) Return loss, b) Reflection coefficient.

Table 2

Return losses, theoretical and experimental.

FREQ. GHz	30Ω	40Ω	75Ω	100Ω
.990	-10.8 ∠-126 -13.2 ∠-125 -11.2	-17.6 ∠-123 -19.2 ∠-123 -18.3	-13.9 ∠ 56 -14.6 ∠ 57 -13.7	-9.1 ∠ 53 -9.6 ∠ 54 -9.4
2.025	-6.8 ∠-160 -8.9 ∠-159 -6.9	-13.1 ∠-157 -14.7 ∠-157 -13.3	-9.5 ∠ 23 -10.1 ∠ 24 -9.5	-5.3 ∠ 21 -5.7 ∠ 22 -5.4
4.005	-8.6 ∠ 140 -10.8 ∠ 139 -8.9	-14.9 ∠ 138 -16.5 ∠ 138 -15.3	-10.7 ∠-37 -11.4 ∠-37 -11.1	-6.1 ∠-32 -6.6 ∠-33 -6.6
8.010	-6.4 ∠-179 -8.3 ∠-179 -6.4	-12.5 ∠-176 -14.0 ∠-176 -12.6	-8.9 ∠ 10 -9.5 ∠ 10 -9.4	-4.9 ∠ 11 -5.3 ∠ 12 -5.2
12.015	-8.9 ∠-141 -10.8 ∠-139 -8.8	-15.9 ∠-133 -17.4 ∠-133 -16.4	-14.3 ∠ 57 -14.8 ∠ 57 -14.7	-10.7 ∠ 59 -11.1 ∠ 60 -10.3

→ Mode Matching
→ Trans. Line
→ Measured

Magnitude dB ∠ (degrees)

types of discontinuities and impedance transformations in finline as well as microstrip.

REFERENCES

[1] J. Smetana, E.G. Farr, and R. Mittra, "Characterization of MMIC devices for active array applications," NASA Technical Memorandum 86907, September, 1984.

[2] E.O. Hammerstad, "Equations for microstrip design," Proc. European Microwave Conference, Hamburg, pp. 268-272, September 1975.

[3] E.G. Farr, Ph.D. Dissertation, to be published.

[4] Wiltron Co., K-Connector catalog, 1984.

[5] W. Oldfield, "ECM/EW designs to 40 GHz in coax," Microwave System News, June 1984.

[6] W. Oldfield, Wiltron Co., personal communication.

[7] E.H. England, "A Coaxial to microstrip transition," IEEE Trans. Microwave Theory Tech., Vol. MTT-24, No. 1, pp. 47-48, jan. 1976.

[8] S.A. Ramo, J.R. Whinnery, and T. Van Duzer, Fields and Waves in Communication Electronics, New York: J. Wiley and Sons, 1984, pp. 214-215.

[9] Wiltron Co., op. cit. p. 2.